Macromolecules

pubs.acs.org/Macromolecules Article

Mapping Chemical Structure−Glass Transition Temperature Relationship through Artificial Intelligence

Luis A. Miccio* and Gustavo A. Schwartz*

Cite This: https://dx.doi.org/10.1021/acs.macromol.0c02594 Read Online

ACCESS | Metrics & More | Article Recommendations | Supporting Information

Downloaded via CSIC on February 5, 2021 at 19:23:53 (UTC).
See https://pubs.acs.org/sharingguidelines for options on how to legitimately share published articles.

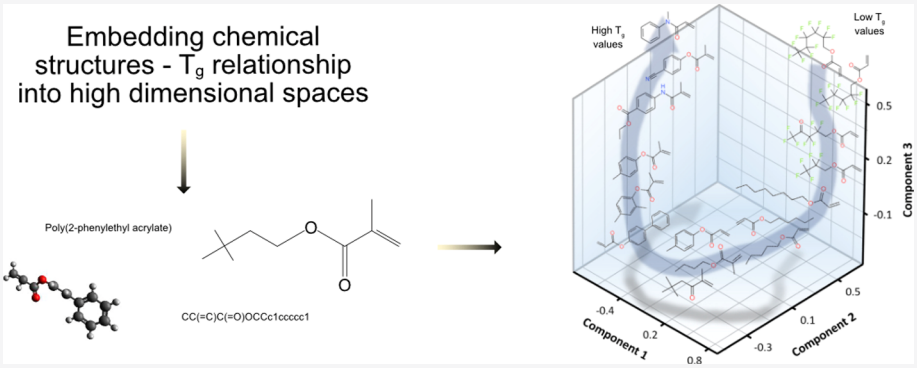

ABSTRACT: Artificial neural networks (ANNs) have been successfully used in the past to predict different properties of polymers based on their chemical structure and to localize and quantify the intramonomer contributions to these properties. In this work, we propose to move forward in order to use the mathematical framework of the ANN for embedding the chemical structure of monomers into a high-dimensional abstract space. This approach allows us not only to accurately predict the glass transition temperature (T_g) of polymers but, even more important, also to encode their chemical structure as *m*-dimensional vectors in a mathematical space. For this aim, we employed a fully connected neural network trained with a set of more than 200 atactic acrylates that provide the coordinates of the vectorized chemical structures into the *m*-dimensional space. These data points were then treated with a hierarchical nonparametric clusterization method in order to automatically group similar chemical structures into clusters with alike properties. These clusters were then projected into a human-readable three-dimensional space using principal component analysis. This approach allows us to deal with chemical structures as if they were mathematical entities and therefore to perform quantitative operations, so far hardly imaginable, being essential for both the design of new materials and the understanding of the structure−property relationships.

■ INTRODUCTION

Quantitative structure−property relationship (QSPR) models have been successfully used for understanding, designing, and predicting material properties[1−10] (glass transition temperature, boiling point, or partition coefficients, among many others). They are based on the premise that the chemical structure of materials is largely related to their properties, and therefore, materials with chemically similar structures will have similar observed properties. Although this is a rather plausible premise, the lack of quantitative methods for comparing chemical structures becomes difficult to properly exploit these structure−property relationships. What do similar chemical structures mean? How can we measure how close two polymers are in terms of their chemical composition? Here, we propose to combine different machine learning techniques for embedding monomer's chemical structures into high-dimensional spaces where quantitative mathematical operations with chemical structures are possible.

Among the many QSPR models, the case of artificial neural networks (ANNs)[5,8,11,12] is particularly interesting because they can "learn to be sensitive to" the chemical structure of polymers, therefore being able to predict related properties. Beyond their success to accurately predict different polymer properties,[7,12−14] in many cases, ANNs just act as black boxes where properly codified information is fed into the network and a given output value is obtained in return.[15,16] In order to tackle the lack of transparency of these methods, we have recently proposed to find and explicitly show the relationship between the features extracted by the ANN from the chemical structure and the

Received: November 20, 2020
Revised: January 22, 2021

 © XXXX American Chemical Society

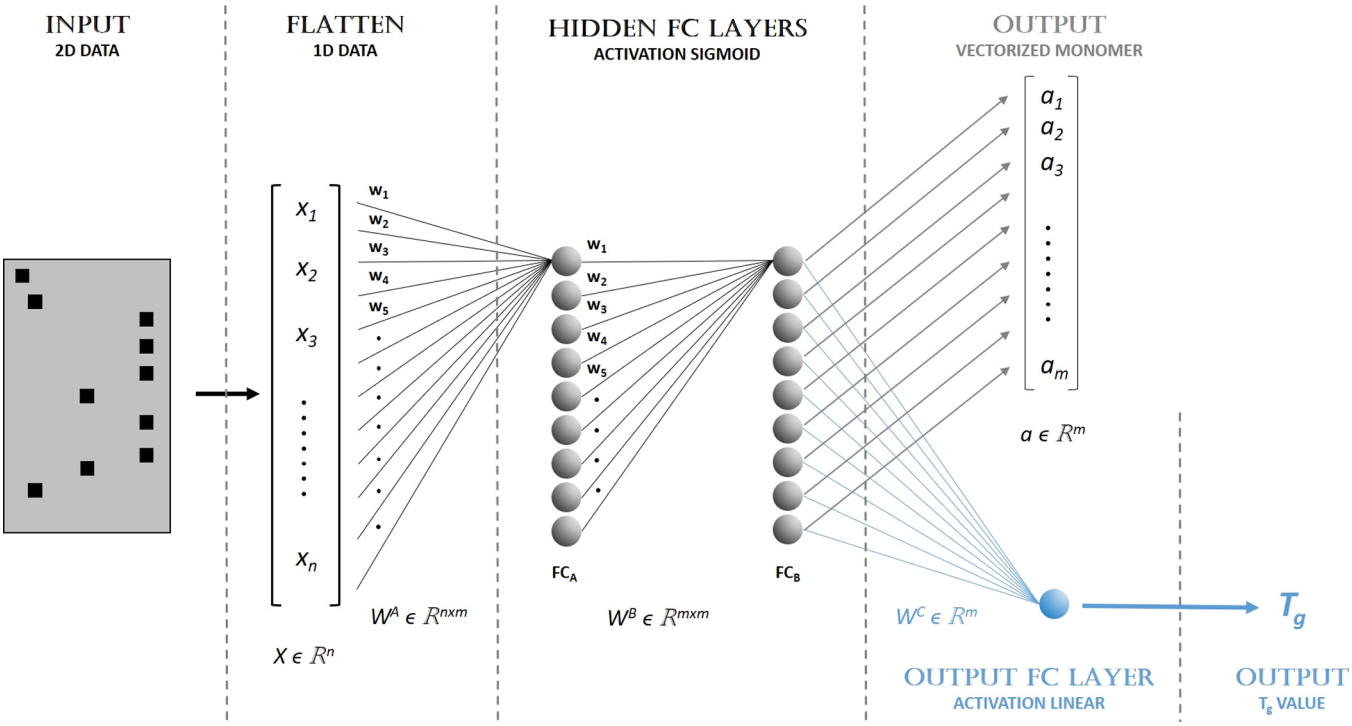

Figure 1. Schematic picture of the ANN employed for embedding the chemical structures.

observed polymer property. In this way, we were able to localize and quantify the intramonomer contributions to the glass transition temperature,[14] based on the assumption that the ANN is able to extract and codify specific features of the chemical structure related to a given polymer property.

In this work, we propose to take a step further in the description of the structure−property relationship "seen" by the ANNs. We exploit the way in which the ANN codifies the chemical structure in order to embed such information into a high-dimensional space where each monomer is represented by an m-dimensional vector. This embedding of the chemical structure of the monomers into a mathematical vector space allows us to perform quantitative operations among them, hardly imaginable until now. For instance, this method allows us to quantify the "distance" between two chemical structures in relation to a given property or to find clusters of monomers with similar properties. This procedure requires constructing adequate visualizations of these m-dimensional vectors into two-dimensional (2D) and three-dimensional (3D) spaces to gain insight into the relationship between monomer structures and the observed final material properties.

In order to obtain proof-of-concept results, we have employed a data set composed of more than 200 atactic acrylates.[14] We have chosen to use the glass transition temperature as a suitable property to validate our approach due to the extensive amount of available data and literature. After training the ANN with this data set, we can obtain T_g-based "coordinates" for each chemical structure in an m-dimensional space. From this high-dimensional representation, we will see how clusterization automatically recognizes similar chemical structures and also how properties of unexplored materials can be estimated.

■ METHODS

In this section, we explain the operations performed on the data in order to accomplish the embedding of the chemical structures, the clusterization process, and the corresponding 3D visualizations.

Data set and Encoding. We used a data set composed of nearly 200 atactic polyacrylates, each of them with their corresponding T_g value[14] (see Table S1) above the molecular weight saturation. The chemical structure of the monomers was transformed into linear strings using SMILES. Then, we converted these strings into binary matrices using a one-hot encoding algorithm[17] and an appropriated dictionary. This encoding was successfully used in previous studies, and the details of this process were published elsewhere.[13,14]

ANN's Architecture. We used fully connected neural networks, fed with the polyacrylate chemical structure codified into binary matrices and the corresponding glass transition temperature (T_g) value. Figure 1 shows a schematic view of the ANN's architecture: after codifying the monomer structure into a 2D matrix, it is then flattened into a one-dimensional vector ($X \in R^n$); this vector is fed to two fully connected layers (FC_A and FC_B) with a varying number of neurons, along with sigmoid activations. Finally, the last hidden layer (FC_B) is connected to a single neuron (layer C) with a linear activation function which provides the predicted glass transition temperature value. The most efficient architecture for the here-studied case consists of 20 neurons on FC_A and FC_B.

ANN's Optimization. As carried out in previous studies,[13,14] to ensure equal weighting of low and high T_g data values during training, the loss function was defined as the average relative error between the actual (A_i) and forecasted (F_i) glass transition temperatures.

$$\text{Loss} = \frac{100}{m_x} \cdot \sum_{i=1}^{m_x} \left(\frac{A_i - F_i}{A_i} \right)$$

From the observed relative difference, the network then recalculates all the weight coefficients through backpropagation.[18] The entire process is repeated several times, until the error achieves a stationary minimum value. In order to achieve the best possible performance for the ANNs before extracting the embedded chemical structures, different values of the network hyperparameters were explored. In this way, several networks with varying parameter values were trained and compared. This comparison was based on the raw performance (minimum relative error) achieved on the data set. Details about the optimization process were given in previous studies.[13,14] For the optimal hyperparameters, Figure 2 shows the excellent agreement

https://dx.doi.org/10.1021/acs.macromol.0c02594
Macromolecules XXXX, XXX, XXX−XXX

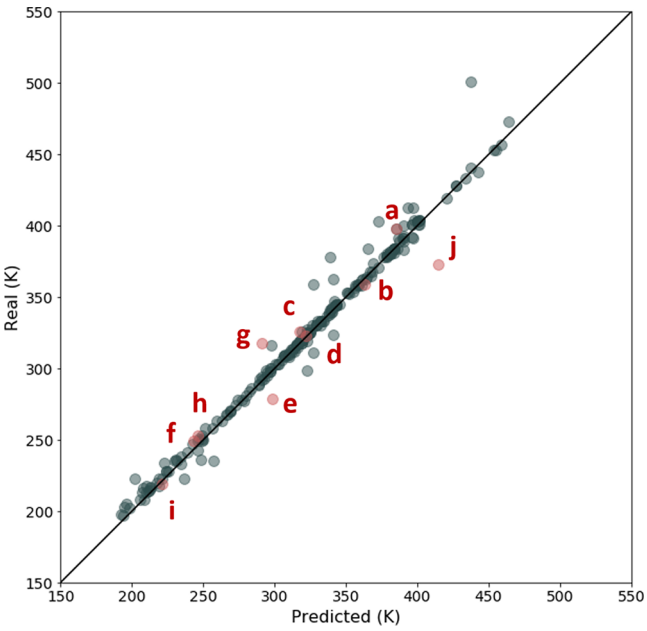

Figure 2. Real *vs* predicted T_g values obtained from the trained ANN. Blue and red dots stand for train and control values, respectively.

between measured and predicted values of the T_g for the whole dataset (including the control group).

Embedding. As shown in Figure 1, a vectorized output (where each component of the vector is given by the corresponding neuron activation value) can be extracted from the last hidden layer of the ANN for every monomer structure. This *m*-dimensional vector represents the embedding of each chemical structure into a high-dimensional vector space. These values are the result of the gradient descent performed during training and are also the input from which the linear activation in the last neuron estimates the T_g value. It is therefore reasonable to assume that they enclose relevant information about the structure learned during weight optimization[14] and can, in turn, be employed as coordinates that define the location of the monomers in this *m*-dimensional space, where chemically similar monomers tend to be closer to each other.

Clustering. It is possible to automatically organize a set of data into groups in such a way that a given property is more similar among the elements of a given group than it is to the elements in other groups. This process is commonly called clustering (or clusterization) and assumes that there are features in the data that would allow distinguishing between these different groups. There are many clustering techniques,[19−25] although there is no universally appropriated one and the best option depends on the nature of the data set under study. Given our aim of capturing the chemical structure−properties related features in our data set and that some structures can deviate from the general behavior trend, we decided to use a hierarchical nonparametric clusterization method called hierarchical density-based spatial clustering of applications with noise (HDBSCAN).[25] This method allows detecting clusters with arbitrary shape and size, different densities, and with the presence of noise or outliers. In addition, no previous assumptions about the number of clusters need to be carried out (which is especially important, given the high dimensionality of our data). In summary, we are therefore defining the clusters as highly dense regions separated by sparse regions in an *m*-dimensional chemical structure−property space.

Visualization. Although we can perform mathematical operations with the vectorized materials in an *m*-dimensional space (such as clusterization), the corresponding visualization becomes impossible for humans in such high-dimensional spaces. In order to gain insight into the learned features, we need to visualize the high-level representations (*m*-dimensional space coordinates) by projecting them into a human-readable 2D or 3D space. In such a way, it is possible to construct

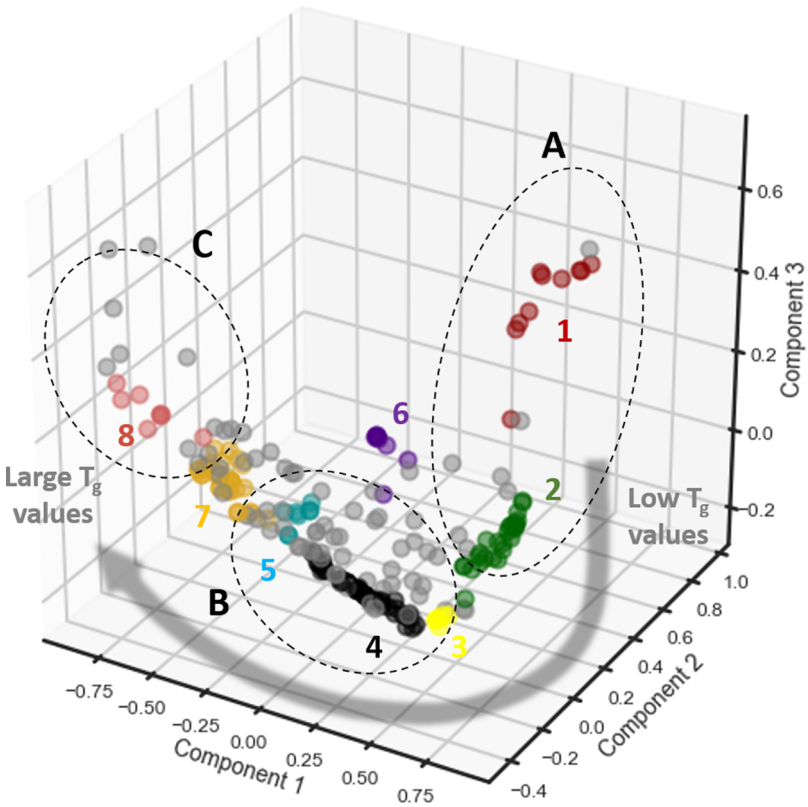

Figure 3. 3D visualization from PCA of the embedded monomers. The arrow and the labeled dashed circles are just a guide for the eyes and show the direction of increasing T_g values and selected regions of the glass transition space, respectively.

https://dx.doi.org/10.1021/acs.macromol.0c02594
Macromolecules XXXX, XXX, XXX−XXX

Table 1. Summary of the Chemical Structure Clusterization

Region	Cluster	Representative input structure	Details
A	1	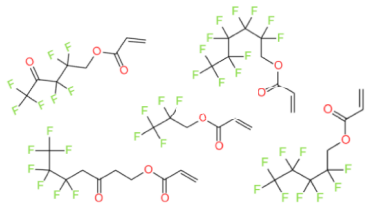	Low observed T_g values when linear chains are present in the monomer's tail and no species adjacent to the reactive group. In particular, the region is predominantly occupied by monomers with no adjacent species (i.e. poly-acrylates) and linear moieties (i.e. carbonated or fluorinated chains).
	2	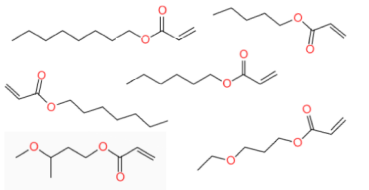	
B	3	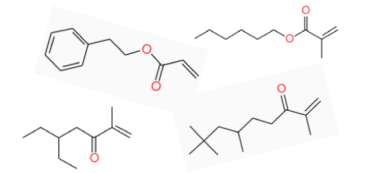	Intermediate observed T_g values as different features are combined in the same monomer structure, thus compensating each other. Therefore, this region is characterized by mixed chemical structures, methacrylates with longer linear moieties, or acrylates with semi-stiff ones (like phenyl groups in linear chains).
	4	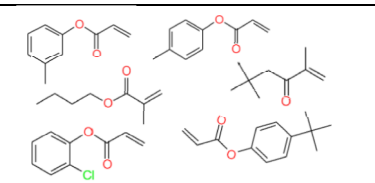	
	5	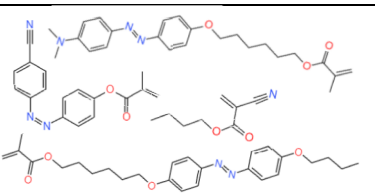	
C	7	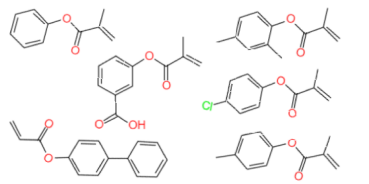	High observed T_g values when phenyl groups are introduced in the monomer's tail and methyl groups are present adjacent to the reactive group. Mainly occupied by both very stiff backbones (with the short methyl group of the methacrylates) and side tails (with phenyl and biphenyl groups).
	8	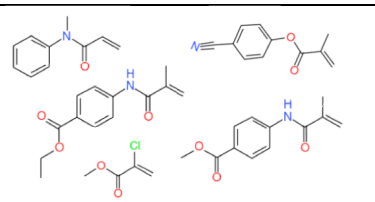	

https://dx.doi.org/10.1021/acs.macromol.0c02594
Macromolecules XXXX, XXX, XXX−XXX

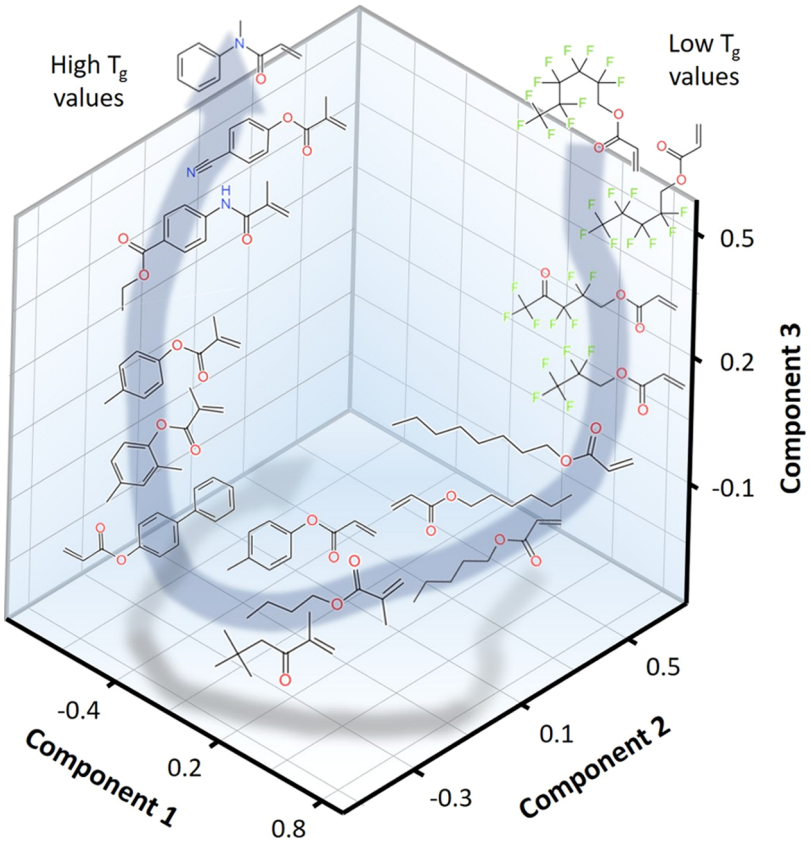

Figure 4. Scheme of the position of selected monomers in the projected 3D space. The arrow is just a guide for the eyes and shows the direction of increasing T_g.

adequate visualizations of the embedded monomer's structure and to study the characteristics of the observed features.

This process was performed using principal component analysis (PCA). PCA is an orthogonal linear transformation that projects the higher dimensional data into a new coordinate system (in a lower dimensional space) in such a way that the first component follows the direction of greatest variance, while the second and third components follow the direction of the second and third greatest variance. Despite the inherent simplicity of the method, it allows a view of the relative position of each chemical structure in a lower dimensional space, generally keeping most of the data variance. In our case, nearly 90% of all variance is kept within the first three components, thus indicating that a 3D representation of the chemical structure−T_g space holds most of the information that the ANN has learned.

Numerical Calculations. After determining the best set of hyperparameters for the ANN, we trained the network obtaining average relative errors for the prediction of the T_g in the range of 3% for both the training and the test sets. No overfitting or relevant systematic differences between train and test errors were observed. It is worth to emphasize here that we are feeding the network only with the chemical structure of the monomer without any other physical or chemical data (either measured or calculated) except the value of the glass transition temperature as output data. Figure 2 shows real versus predicted values for the train (blue dots) and control (labeled red dots) sets obtained after training our fully connected ANN. As shown, the trained ANN predicts the external control group glass transition temperatures quite well, even for a wide range of chemical structures. The corresponding control group chemical structures are presented in Figure S1.

Despite the so-obtained low errors, our aim is not only to predict the T_g but also to have a method for embedding the molecular structure of the monomers into an m-dimensional space (m = 20) where we can quantitatively describe the chemical structure and compare it to other structures. Similar chemical structures are expected to form clusters well separated from other groups with different chemical characteristics. After clustering the embedded chemical structures, we projected the data into a 3D representation for easier visualization.

■ DISCUSSION

Figure 3 shows the PCA projection of the m-dimensional space into a 3D representation. Each dot represents a monomer structure where different dot colors account for the different clusters as obtained after applying the HDBSCAN method. Gray dots indicate "noise", that is, monomer structures which were not included in any cluster. Interestingly, data points in Figure 3 can be seen as approximately located on an imaginary "path" which starts in the upper-right corner (labeled region A), goes down and left (through region B), and ends in the upper-left corner (region C). This path also indicates increasing values of T_g. While the embedding process carried out by the ANN allows a representation of each monomer as a dot in an m-dimensional space and, in turn, the PCA allows a visualization of these dots into a human-readable 3D space, clusterization is responsible for labeling these monomers as a part (or not) of each group. Thus, polymers within each cluster have both a similar chemical structure and similar values of T_g.

Table 1 shows the clusters belonging to each of the regions highlighted in Figure 3 (A, B, and C), as obtained using the HDBSCAN method, together with some typical chemical structures observed in each group. These results show that the ANN can efficiently learn and quantitatively locate in space the chemically meaningful features associated with the glass transition temperature. In this way, since each monomer location is related to the chemical structure−T_g relationship, we can take a step forward and build a scheme where each structure is shown at different locations in the projected 3D

https://dx.doi.org/10.1021/acs.macromol.0c02594
Macromolecules XXXX, XXX, XXX−XXX

space, as the one presented in Figure 4. As shown, long linear chains mainly occupy the upper-right side of the figure (region labeled A in Figure 3, which also corresponds to the clusters 1 and 2). As the chains get stiffer or a methyl group is present next to the reactive group (*i.e.,* methacrylate), the monomers progressively move down and to the center of the space (*i.e.,* the region labeled B in Figure 3 and corresponding to clusters 3, 4, and 5 in the same figure). In this region, several feature combinations can be observed, such as very stiff backbones with no side groups (like phenyl or short linear tail acrylates). In the upper-left side of the projected space, that is, the place where the chemical structures with higher glass transition temperatures are located, the observed structures present very stiff backbones and side groups. A complete list of the monomers contained in each of the clusters is presented in the Supporting Information (see Table S2). It is also noteworthy that many monomers are labeled as noise during the clusterization process which means that they cannot be assigned to any cluster with certainty. Although there are monomers that present similar chemical features to some of the clustered ones, such a similarity seems to be compensated by the presence of other chemical features that drive the overall chemical structure and glass transition temperature value in a different direction. Therefore, the similarities are not enough to fit into the corresponding cluster. Representative chemical structures in the noise are also presented in the Supporting Information (see Figure S2), along with the employed clustering parameters. The clusterization process is therefore automating the recognition process of both the noise and the different groups of polymers (linked to each other by chemical similarities and observed glass transition temperatures).

From a chemical point of view, the clusterization process can be rationalized by analyzing the chemically relevant features for the here-studied monomers as follows: on the one hand, we have units with species adjacent to the monomer's functional group (*e.g.,* the methyl group in methacrylates increases T_g). These species produce changes in the backbone stiffness of the polymer.[26−28] This effect is diluted as the monomer's tail increases in size, as observed for poly(pentyl methacrylate) and poly(hexyl methacrylate) in cluster 3 and poly(butyl methacrylate), poly(*sec* butyl methacrylate), and poly(neo pentyl methacrylate) in cluster 4. On the other hand, we have to take into account size, shape, and stiffness of the side groups (or "tail"): the larger the volume occupied by a rigid tail, the higher the observed glass transition temperature (see also the tail-adjacent scheme in Figure S1). Therefore, short and ramified groups tend to increase T_g, while long and linear ones tend to decrease it (lubricating effect).[29,30] In particular, the glass transition temperature decreases with the number of carbons in the ester group because of the increased bulk of the side chain as observed for poly(1*H*,1*H*-pentafluoropropyl acrylate), poly(1*H*,1*H*,3*H*-hexafluorobutyl acrylate), poly(1*H*,1*H*,5*H*-octafluoropentyl acrylate), poly(1*H*,1*H*-undecafluorohexyl acrylate), and poly(2,2,3,3,5,5,5-heptafluoro-4-oxapentyl acrylate) in cluster 1 and poly(*n*-pentyl acrylate), poly(hexyl acrylate), poly(heptyl acrylate), and poly(octyl acrylate) in cluster 2. However, after observing a minimum, the T_g effect is masked by entanglements,[31] and the T_g starts increasing again. Polymers with fluorinated ester groups have higher glass transition temperatures than polymers with nonfluorinated alkyl groups of the same carbon chain length.[31,32]

It is worth mentioning here that no *a priori* assumptions about the role of the interchain interactions on the T_g were made. In principle, intermolecular contributions are implicitly related to the monomer chemical structure (*i.e.,* the repeating unit that constitutes the polymer chains), and therefore, it is indirectly "seen" by the ANN. In summary, we have shown the ANN capability of detecting and embedding the chemical structure of the monomers and the power of the automatic clusterization of the embedded monomer structures which locate similar monomers close to each other in order to separate similar contributions to the glass transition temperature.

CONCLUSIONS

In this work, we have trained an ANN for embedding the chemical structure of monomers into a high-dimensional space. We have shown that the vectorized chemical structures so obtained can be mathematically manipulated. In particular, we have also demonstrated that the vectorized representation of the monomers can be automatically separated into different sets using a hierarchical density-based clustering technique in order to group them by their chemical affinity. In addition, this clusterization can also be visualized into a human-readable 3D space by applying a linear projection (PCA). This mathematical representation of the monomer's chemical structure can be of valuable help for understanding the properties of polymers and for designing new materials. Finally, it is worth to remind here that this approach relies only on the knowledge of the chemical formula of the repeating unit and does not require any kind of experimental data or calculations as the input.

ASSOCIATED CONTENT

Supporting Information

The Supporting Information is available free of charge at https://pubs.acs.org/doi/10.1021/acs.macromol.0c02594.

Data set glass transition temperatures, control group composition and chemical structures, list and composition of clusters, and noise composition and chemical structure (PDF)

AUTHOR INFORMATION

Corresponding Authors

Luis A. Miccio − *Centro de Física de Materiales (CSIC-UPV/EHU)-Materials Physics Center (MPC), 20018 San Sebastián, Spain; Donostia International Physics Center, 20018 San Sebastián, Spain; Institute of Materials Science and Technology (INTEMA), National Research Council (CONICET), 7600 Mar del Plata, Buenos Aires, Argentina;* orcid.org/0000-0002-3942-1908; Email: lamiccio@gmail.com

Gustavo A. Schwartz − *Centro de Física de Materiales (CSIC-UPV/EHU)-Materials Physics Center (MPC), 20018 San Sebastián, Spain; Donostia International Physics Center, 20018 San Sebastián, Spain;* orcid.org/0000-0003-3044-2435; Email: gustavo.schwartz@csic.es

Complete contact information is available at: https://pubs.acs.org/10.1021/acs.macromol.0c02594

Author Contributions

The manuscript was written by L.A.M. and G.A.S. Both authors have given approval to the final version of the manuscript.

Notes

The authors declare no competing financial interest.

■ ACKNOWLEDGMENTS

We gratefully acknowledge the financial support from the Spanish Government "Ministerio de Ciencia e Innovación" (PID2019-104650GB-C21) and the Basque Government (IT-1175-19). We also acknowledge the support of NVIDIA Corporation with the donation of the Titan V GPU used for this research.

■ REFERENCES

(1) Joyce, S. J.; Osguthorpe, D. J.; Padgett, J. A.; Price, G. J.; Ba, Y. Neural Network Prediction of Glass-transition Temperatures from Monomer Structure. *J. Chem. Soc., Faraday Trans.* **1995**, *91*, 2491−2496.

(2) Ulmer, C. W.; Smith, D. A.; Sumpter, B. G.; Noid, D. I. Computational neural networks and the rational design of polymeric materials: the next generation polycarbonates. *Comput. Theor. Polym. Sci.* **1998**, *8*, 311−321.

(3) Schwartz, G. A. Prediction of Rheometric Properties of Compounds by Using Artificial Neural Networks. *Rubber Chem. Technol.* **2001**, *74*, 116−123.

(4) Mattioni, B. E.; Jurs, P. C. Prediction of Glass Transition Temperatures from Monomer and Repeat Unit Structure Using Computational Neural Networks. *J. Chem. Inf. Comput. Sci.* **2002**, *42*, 232−240.

(5) Zhang, Z.; Friedrich, K. Artificial neural networks applied to polymer composites: a review. *Compos. Sci. Technol.* **2003**, *63*, 2029−2044.

(6) Bertinetto, C.; et al. Prediction of the glass transition temperature of (meth) acrylic polymers containing phenyl groups by recursive neural network. *Polymer* **2007**, *48*, 7121−7129.

(7) Liu, W.; Cao, C. Artificial neural network prediction of glass transition temperature of polymers. *Colloid Polym. Sci.* **2009**, *287*, 811−818.

(8) Liu, Y.; Zhao, T.; Ju, W.; Shi, S. Materials discovery and design using machine learning. *J. Materiomics* **2017**, *3*, 159−177.

(9) Hou, F.; et al. Comparison Study on the Prediction of Multiple Molecular Properties by Various Neural Networks. *J. Phys. Chem. A* **2018**, *122*, 9128−9134.

(10) Toropov, A. A.; Toropova, A. P.; Kudyshkin, V. O.; Bozorov, N. I.; Rashidova, S. S. Applying the Monte Carlo technique to build up models of glass transition temperatures of diverse polymers. *Struct. Chem.* **2020**, *31*, 1739−1743.

(11) Jiang, Z.; Zhang, Z.; Friedrich, K. Prediction on wear properties of polymer composites with artificial neural networks. *Compos. Sci. Technol.* **2007**, *67*, 168−176.

(12) Zheng, X.; Zheng, P.; Zheng, L.; Zhang, Y.; Zhang, R.-Z. Multi-channel convolutional neural networks for materials properties prediction. *Comput. Mater. Sci.* **2020**, *173*, 109436.

(13) Miccio, L. A.; Schwartz, G. A. From chemical structure to quantitative polymer properties prediction through convolutional neural networks. *Polymer* **2020**, *193*, 122341.

(14) Miccio, L. A.; Schwartz, G. A. Localizing and quantifying the intra-monomer contributions to the glass transition temperature using artificial neural networks. *Polymer* **2020**, *203*, 122786.

(15) Sha, W.; Edwards, K. L. The use of artificial neural networks in materials science based research. *Mater. Des.* **2007**, *28*, 1747−1752.

(16) Duan, Z. H.; Kou, S. C.; Poon, C. S. Prediction of compressive strength of recycled aggregate concrete using artificial neural networks. *Constr. Build. Mater.* **2013**, *40*, 1200−1206.

(17) Alkharusi, H. Categorical Variables in Regression Analysis: A Comparison of Dummy and Effect Coding. *Int. J. Educ.* **2012**, *4*, 202−210.

(18) Rumelhart, D. E.; Hinton, G. E.; Williams, R. J. Learning representations by back-propagating errors. *Nature* **1986**, *323*, 533−536.

(19) Jin, X.; Han, J. K-Means Clustering. *Encyclopedia of Machine Learning and Data Mining*; Springer US, 2017; pp 695−697.

(20) Ward, J. H. Hierarchical Grouping to Optimize an Objective Function. *J. Am. Stat. Assoc.* **1963**, *58*, 236−244.

(21) Herbin, M.; Bonnet, N.; Vautrot, P. Estimation of the number of clusters and influence zones. *Pattern Recognit. Lett.* **2001**, *22*, 1557−1568.

(22) Hinneburg, A.; Keim, D. A. A General Approach to Clustering in Large Databases with Noise. *Knowl. Inf. Syst.* **2003**, *5*, 387−415.

(23) Stuetzle, W.; Nugent, R. A generalized single linkage method for estimating the cluster tree of a density. *J. Comput. Graph. Stat.* **2010**, *19*, 397−418.

(24) Naldi, M. C.; Campello, R. J. G. B.; Hruschka, E. R.; Carvalho, A. C. P. L. F. Efficiency issues of evolutionary k-means. *Appl. Soft Comput.* **2011**, *11*, 1938−1952.

(25) Campello, R. J. G. B.; Moulavi, D.; Sander, J. Density-based clustering based on hierarchical density estimates. *Advances in Knowledge Discovery and Data Mining*; Lecture Notes in Computer Science (including subseries Lecture Notes in Artificial Intelligence and Lecture Notes in Bioinformatics); Springer: Berlin, 2013; Vol. *7819* LNAI, pp 160−172.

(26) Gibbs, J. H. Nature of the glass transition in polymers. *J. Chem. Phys.* **1956**, *25*, 185−186.

(27) Gibbs, J. H.; DiMarzio, E. A. Nature of the glass transition and the glassy state. *J. Chem. Phys.* **1958**, *28*, 373−383.

(28) Fox, T. G.; Flory, P. J. Second-order transition temperatures and related properties of polystyrene. I. Influence of molecular weight. *J. Appl. Phys.* **1950**, *21*, 581−591.

(29) Overberger, C. G.; Arond, L. H.; Wiley, R. H.; Garrett, R. R. Monomers containing large alkyl groups. IV. Polymerization and properties of the polymers of 2-alkyl-1,3-butadienes. *J. Polym. Sci.* **1951**, *7*, 431−441.

(30) Jordan, E. F.; Feldeisen, D. W.; Wrigley, A. N. Side-chain crystallinity. I. Heats of fusion and melting transitions on selected homopolymers having long side chains. *J. Polym. Sci., Part A-1: Polym. Chem.* **1971**, *9*, 1835−1851.

(31) Gaynor, J.; Schueneman, G.; Schuman, P.; Harmon, J. P. Effects of fluorinated substituents on the refractive index and optical radiation resistance of methacrylates. *J. Appl. Polym. Sci.* **1993**, *50*, 1645−1653.

(32) Miccio, L. A.; Liaño, R.; Montemartini, P. E.; Oyanguren, P. A. Partially fluorinated polymer networks: Synthesis and structural characterization. *J. Appl. Polym. Sci.* **2011**, *122*, 608−616.

https://dx.doi.org/10.1021/acs.macromol.0c02594
Macromolecules XXXX, XXX, XXX−XXX